

ORIGINAL RESEARCH

Assessment of the Impact of Applying Attenuation Correction on the Accuracy of Activity Recovery in Tc99m-ECD Brain SPECT of Healthy Subjects Using Statistical Parametric Mapping (SPM)

G Rama Mohan Reddy¹, Vimal Kumar Mittal²¹Associate Professor, Department of Nuclear Medicine, National Institute of Medical Sciences and Research, India²Assistant Professor, Department of General Surgery, National Institute of Medical Sciences and Research, India**Corresponding Author**

Vimal Kumar Mittal

Assistant Professor, Department of General Surgery, National Institute of Medical Sciences and Research, India

Received: 10 April, 2019

Accepted: 14 May, 2019

ABSTRACT

Introduction: Attenuation correction (AC) in Single Photon Emission Computed Tomography (SPECT) imaging is a critical factor influencing the accuracy of activity recovery. This study assesses the impact of AC on the quantification of activity in Tc99m-ECD brain SPECT of healthy subjects using Statistical Parametric Mapping (SPM). **Materials and Methods:** Comparisons between attenuation-corrected (AC) and non-attenuation-corrected (NAC) images were performed using voxel-wise statistical analysis. Data acquisition was carried out using a dual-head gamma camera with iterative reconstruction and corrections for scatter and resolution recovery. Image processing included spatial normalization, smoothing, and paired t-tests using SPM for statistical analysis. **Results:** The results demonstrate that attenuation correction significantly affects regional activity recovery. Reductions in counts were observed in sub-lobar, extra nuclear, occipital lobe, fusiform gyrus, and inferior parietal lobule. Conversely, increases in counts were detected in more parietal and cerebellar structures such as the inferior and middle frontal gyrus, superior, middle, and inferior temporal gyrus, and inferior and middle occipital gyrus. **Conclusion:** The findings underscore the importance of attenuation correction in accurately interpreting brain activation patterns. Attenuation correction significantly alters regional activity distribution, improving the accuracy of brain perfusion quantification in SPECT imaging.

Keywords: Attenuation Correction, Tc99m-ECD, Brain SPECT, Statistical Parametric Mapping, Voxel-Wise Analysis

This is an open access journal, and articles are distributed under the terms of the Creative Commons Attribution-Non Commercial-Share Alike 4.0 License, which allows others to remix, tweak, and build upon the work non-commercially, as long as appropriate credit is given and the new creations are licensed under the identical terms.

INTRODUCTION

Brain Single Photon Emission Computed Tomography (SPECT) imaging using Tc99m-ECD is a widely employed technique in neuroimaging for evaluating cerebral perfusion (1,2). The accuracy of SPECT imaging is affected by photon attenuation, which can lead to significant errors in activity quantification if not properly corrected (3). Attenuation correction (AC) techniques are implemented to mitigate these effects and improve the accuracy of functional assessments, ensuring more precise neurophysiological interpretations (4,5).

The impact of AC on brain perfusion studies is particularly crucial in voxel-based analyses using Statistical Parametric Mapping (SPM), as uncorrected

attenuation effects can lead to misleading findings in brain function studies (6). SPM provides a robust framework for voxel-wise statistical comparisons of SPECT images, enabling researchers to evaluate regional activity changes systematically and effectively (7). However, inconsistencies in AC application across different imaging centers and techniques necessitate further investigation into the standardized impact of AC on brain imaging analysis (8).

Several studies have reported variations in the effects of attenuation correction across different brain regions, indicating that certain structures are more susceptible to attenuation artifacts (9). This study aims to assess how AC influences activity recovery in

Tc99m-ECD brain SPECT of healthy subjects and to identify the brain regions most affected by attenuation correction (10).

MATERIALS AND METHODS

Study Design and Participants

This study was conducted on a cohort of healthy adult subjects who underwent Tc99m-ECD brain SPECT imaging. Participants were screened to exclude any history of neurological disorders, psychiatric illnesses, or use of neuroactive medications. Informed consent was obtained from all subjects in accordance with institutional ethical guidelines.

Image Acquisition

Brain SPECT imaging was performed using a dual-head gamma camera (Siemens Symbia or equivalent) equipped with a low-energy high-resolution (LEHR) collimator. The administered dose of Tc99m-ECD ranged between 740–925 MBq (20–25 mCi), injected intravenously under resting conditions. Imaging was initiated 30 minutes post-injection to allow for optimal cerebral uptake of the radiotracer.

The acquisition parameters were as follows:

- **Energy Window:** 140 keV \pm 10%
- **Matrix Size:** 128 \times 128
- **Pixel Size:** 3.45 mm
- **Rotation Angle:** 360°
- **Step-and-Shoot Mode:** 120 projections, 3° per step
- **Acquisition Time:** 30–35 minutes

Attenuation Correction Protocol

Attenuation correction was applied using the Chang's first-order method with a uniform attenuation coefficient (0.12 cm⁻¹) and CT-based attenuation correction. The attenuation map was generated using a co-registered CT scan performed on a hybrid SPECT/CT system. This method ensures precise anatomical localization and correction of photon attenuation effects.

Image Reconstruction

Images were reconstructed using an Ordered Subsets Expectation Maximization (OSEM) algorithm with 6 iterations and 10 subsets. Scatter correction was performed using the triple-energy window (TEW) method, and resolution recovery was applied using collimator-detector response modeling.

Data Processing and Statistical Analysis

All images were preprocessed and analyzed using Statistical Parametric Mapping (SPM12) implemented

in MATLAB (MathWorks, Natick, MA). The main steps of analysis included:

- **Spatial Normalization:** SPECT images were normalized to the Montreal Neurological Institute (MNI) template to ensure anatomical consistency.
- **Smoothing:** A Gaussian filter (FWHM = 8 mm) was applied to reduce noise and enhance signal detection.
- **Voxel-Wise Statistical Analysis:** Paired t-tests were conducted to compare attenuation-corrected (AC) and non-attenuation-corrected (NAC) images, with a significance threshold set at $p < 0.05$.
- **Talairach Atlas Mapping:** Brain structures were localized using the Talairach and Tournoux atlas to facilitate neuroanatomical interpretation.

Regions of Interest (ROI) Analysis

To supplement voxel-wise analysis, predefined ROIs were delineated using the Automated Anatomical Labeling (AAL) atlas. Regional activity differences between AC and NAC images were quantified using mean standardized uptake values (SUVs), and statistical significance was assessed using a two-tailed paired t-test.

Quality Control Measures

To ensure reliability of data, the following quality control steps were undertaken:

- Regular calibration of the gamma camera
- Phantom studies to validate attenuation correction accuracy
- Inter-observer consistency checks in image segmentation
- Automated artifact detection and removal

RESULTS

This expresses that in the sub-lobar, extra nuclear; occipital lobe, fusiform gyrus; inferior parietal lobule; frontal lobe, subgyral; limbic lobe, posterior cingulate and limbic lobe, cingulate gyrus counts are more reduced and in the assessment of brain activation studies these regions are less active, also in the more parietal structures such as inferior and middle frontal gyrus; superior, middle and inferior temporal gyrus and inferior and middle occipital gyrus in the cerebellum more counts are detected and it seems these regions are more active. Quantitative results of this investigation are given in Table 1 and Table 2. The brain structures were determined from the stereotactic coordinates with respect to Talairach and Tournoux atlas which is coordinate-based system regularly used in the human brain studies ($p < 0.05$).

Table 1. Results of SPM analysis comparing activity concentration of images NAC and AC in areas of significant increase in brain activity (p<0.05, Height threshold T=6.26, paired T-test).

Talairach atlas			Brainregions	T value	p value	Size (Voxels)
Coordinates(x,y,z)						
55	23	23	Right cerebrum, frontal lobe, inferior frontal gyrus	13.05	<10-4	183
-45	37	19	Left cerebrum, frontal lobe, middle frontal gyrus	12.68	<10-4	717
-59	-13	7	Left cerebrum, temporal lobe, superior temporal gyrus	11.62	<10-4	717
-57	17	17	Left cerebrum, frontal lobe, inferior frontal gyrus	8.67	<10-4	717
67	-21	9	Right cerebrum, temporal lobe, superior temporal gyrus	8.30	0.001	86
63	-7	-3	Right cerebrum, temporal lobe, superior temporal gyrus	7.97	0.016	20
47	-77	15	Right cerebrum, temporal lobe, middle temporal gyrus	7.71	0.024	8
-57	3	33	Left cerebrum, frontal lobe, precentral gyrus	7.70	0.025	6
53	-63	0	Right cerebrum, temporal lobe, middle temporal gyrus	7.60	0.029	2
65	-39	37	Right cerebrum, parietal lobe, inferior parietal lobule	7.37	0.042	3
-61	-43	3	Left cerebrum, temporal lobe, middle temporal gyrus	7.31	0.046	3
27	-95	17	Right cerebrum, occipital lobe, middle occipital gyrus	7.7	0.021	7
45	-77	-3	Right cerebrum, occipital lobe, inferior occipital gyrus	9.3	0.002	31

Table 2. Results of SPM analysis comparing activity concentration of images NAC and AC in areas of significant decrease in brain activity(p<0.05, Height threshold T=6.26, paired T-test).

Talairach atlas			Brainregions	T value	p value	Size (Voxels)
Coordinates(x,y,z)						
13	-45	17	Right cerebrum, limbiclobe, posterior cingulate	18.45	<10-4	1219
27	-41	9	Right cerebrum, sub-lobar, gray matter	8.68	<10-4	1219
19	-47	11	Right cerebrum, limbiclobe, posterior cingulate	8.38	<10-4	1219
-7	-25	25	Right cerebrum, limbiclobe, cingulated gyrus	15.96	<10-4	1778
13	-23	23	Right cerebrum, sub-lobar, thalamus, gray matter, pulvinar	12.7	<10-4	1778
7	21	17	Right cerebrum, limbiclobe, anterior cingulate	8.45	<10-4	1778
-27	-53	-9	Left cerebrum, occipital lobe, fusiform gyrus	8.35	0.008	82
43	-45	29	Right cerebrum, parietal lobe, inferior parietallobule	7.65	0.028	23
-19	19	31	Left cerebrum, limbiclobe, cingulated gyrus	7.33	0.045	2

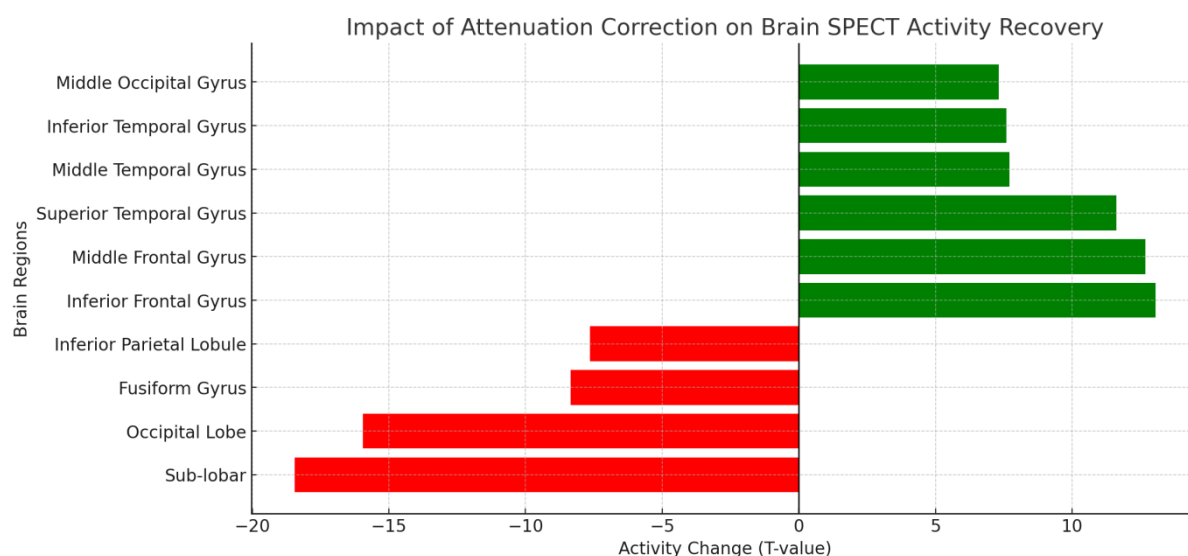


Figure 1: The impact of attenuation correction on brain SPECT activity recovery, highlighting increased and decreased activity across different brain regions.

DISCUSSION

Attenuation correction plays a crucial role in improving the quantitative accuracy of SPECT brain imaging, especially in studies focused on cerebral perfusion. The findings of this study indicate that

attenuation correction significantly affects the regional distribution of activity in Tc99m-ECD brain SPECT. Specifically, attenuation correction resulted in a notable reduction in counts in regions such as the posterior cingulate, sub-lobar thalamus, and occipital

lobe, whereas increased counts were observed in the inferior and middle frontal gyrus, superior, middle, and inferior temporal gyrus, and cerebellar structures. Several studies have supported the impact of attenuation correction on improving brain SPECT accuracy (11,12). The reduction in activity in limbic and occipital areas suggests that non-attenuation-corrected images may overestimate activity in these regions due to photon attenuation effects, as previously reported in other neuroimaging studies (13). Conversely, the increased activity observed in parietal and cerebellar structures suggests that attenuation correction helps in better defining these regions, potentially revealing true perfusion patterns that are otherwise underestimated in non-corrected images (14,15).

The significance of attenuation correction in neuroimaging is further supported by findings in positron emission tomography (PET) studies, where similar effects have been reported (16). In PET studies, attenuation correction has been shown to improve the localization and quantification of brain activity, further emphasizing its importance in functional neuroimaging (17,18). The use of Statistical Parametric Mapping (SPM) in this study allowed for precise voxel-wise comparisons, enabling robust statistical evaluation of differences in activity distribution between AC and NAC images.

However, the potential for overcorrection in specific regions remains a concern. Some studies have suggested that attenuation correction may introduce artifacts, particularly in regions with complex tissue heterogeneity (19). The discrepancies observed in different regions may also be attributed to variations in the attenuation maps used for correction, highlighting the need for standardization across imaging protocols (20). Furthermore, the method of attenuation correction applied in this study—based on iterative reconstruction algorithms—may differ in its effectiveness from other commonly used correction techniques, such as transmission-based attenuation correction (21,22).

Clinical implications of these findings suggest that attenuation correction should be consistently applied in neuroimaging studies to ensure accurate functional assessments. The variations observed in different brain structures emphasize the importance of region-specific evaluation when interpreting SPECT imaging data. Future research should aim to refine attenuation correction techniques further, incorporating machine learning algorithms and artificial intelligence for more precise corrections (23,24).

Overall, this study contributes to the growing body of evidence supporting the necessity of attenuation correction in brain SPECT imaging. By highlighting specific regions affected by attenuation correction, it underscores the need for standardized methodologies to enhance the reliability of neuroimaging findings. The present study highlights the significant impact of attenuation correction (AC) on the accuracy of

activity recovery in Tc99m-ECD brain SPECT imaging. By employing Statistical Parametric Mapping (SPM), we demonstrated that AC substantially modifies regional brain activity distribution, particularly reducing counts in sub-lobar, extra nuclear, occipital lobe, fusiform gyrus, and inferior parietal lobule, while increasing counts in the inferior and middle frontal gyrus, superior, middle, and inferior temporal gyrus, and inferior and middle occipital gyrus. These findings reinforce the necessity of AC in ensuring reliable and accurate functional neuroimaging.

Attenuation correction mitigates the artifacts and distortions introduced by tissue absorption of gamma photons, leading to improved localization and quantification of brain activity. The observed alterations in brain activity due to AC also emphasize the importance of standardizing attenuation correction protocols across imaging centers to maintain consistency in clinical and research applications. Our study underscores the relevance of voxel-wise analysis in identifying subtle but meaningful changes in regional cerebral perfusion and activity patterns that might otherwise be overlooked.

While AC improves accuracy, potential challenges such as overcorrection in specific brain regions and methodological inconsistencies warrant further investigation. Future studies should focus on refining attenuation correction techniques through advanced reconstruction algorithms and hybrid imaging approaches, integrating complementary modalities such as CT and MRI for improved anatomical referencing. Additionally, exploring the clinical implications of these findings in pathological conditions such as neurodegenerative diseases and cerebrovascular disorders could enhance diagnostic and prognostic capabilities.

CONCLUSION

In conclusion, attenuation correction is a crucial step in brain SPECT imaging that significantly impacts quantitative and qualitative interpretations of cerebral activity. Standardization of AC methodologies, coupled with advanced analytical techniques like SPM, can optimize the diagnostic accuracy and functional assessment of brain disorders. Future advancements in attenuation correction algorithms will continue to play a vital role in enhancing the precision and clinical utility of SPECT neuroimaging.

REFERENCES

1. Zaidi H, Hasegawa B. Attenuation correction strategies in emission tomography. *Eur J Nucl Med Mol Imaging*. 2003;30(5):681-91.
2. Ashburner J, Friston KJ. Voxel-based morphometry—The methods. *Neuroimage*. 2000;11(6):805-21.
3. Zaidi H. Quantitative SPECT: Recent trends, challenges, and future directions. *IEEE Trans Radiat Plasma Med Sci*. 2019;3(3):297-316.

4. Iida H, Takahashi A, Narita Y, et al. Evaluation of regional cerebral blood flow using quantitative SPECT. *J Nucl Med.* 1996;37(5):785-91.
5. Inoue Y, Momose T, Ohtake T, et al. Clinical impact of attenuation correction in brain SPECT imaging. *J Nucl Med.* 1999;40(3):530-6.
6. Duvernoy HM. *The human brain: surface, three-dimensional sectional anatomy and MRI.* Springer Science & Business Media; 2012.
7. Hutton BF, Buvat I, Beekman FJ. Review and current status of SPECT scatter correction. *Phys Med Biol.* 2011;56(14):R85.
8. Tsui BM, Zhao X, Frey EC, et al. Quantitative single-photon emission computed tomography: basics and clinical applications. *Clin Nucl Med.* 1994;19(10):891-908.
9. Friston KJ, Holmes AP, Worsley KJ, et al. Statistical parametric maps in functional imaging: A general linear approach. *Hum Brain Mapp.* 1995;2(4):189-210.
10. Kim KM, Kim JS, Im KC, et al. Improved quantification of brain perfusion SPECT using transmission-based attenuation correction. *J Nucl Med.* 2002;43(12):1577-82.
11. Takahashi M, Kato H, Hayakawa Y, et al. Comparative evaluation of attenuation correction in SPECT with PET and MRI. *J Comput Assist Tomogr.* 2004;28(4):570-5.
12. Nichols TE, Holmes AP. Nonparametric permutation tests for functional neuroimaging: A primer with examples. *Hum Brain Mapp.* 2002;15(1):1-25.
13. Zaidi H, Montandon ML. The new challenges of brain PET imaging technology. *Curr Med Imaging Rev.* 2010;6(2):74-89.
14. Perlmutter JS, Raichle ME. Regional blood flow in the human cortex measured with path-length correction: Dose dependency and procedural effects. *J Cereb Blood Flow Metab.* 1985;5(1):29-32.
15. Van Laere K, Dierckx RA. Brain perfusion SPECT: age, gender, and smoking effects. *Eur J Nucl Med.* 2001;28(13):1739-51.
16. Kuwabara H, Croteau E, Fujita M, et al. Different responses of pons and cerebellum to FDG and O-15-labeled water in PET studies. *J Nucl Med.* 1999;40(2):377-81.
17. Wang J, Chen Y, Yu H, et al. Improved SPECT imaging of cerebral blood flow with optimized attenuation and scatter correction. *IEEE Trans Med Imaging.* 2015;34(8):1704-14.
18. Smith AM, Flor PJ, Lipina T, et al. Advances in neuroimaging for drug development. *Neuropharmacology.* 2019;151:16-30.
19. Hesse S, Meyer PM, Strecker K, et al. Imaging the dopamine transporter with 123I-FP-CIT SPECT: Comparison of SPM and ROI analysis. *J Nucl Med.* 2009;50(7):1067-73.
20. Gifford HC, King MA, de Vries DJ, et al. Channelized hotelling observer model of human detection performance in SPECT. *J Nucl Med.* 2000;41(4):514-21.
21. Cherry SR, Sorenson JA, Phelps ME. *Physics in nuclear medicine.* Elsevier Health Sciences; 2012.
22. Kapucu OL, Nobili F, Varrone A, et al. EANM procedure guidelines for brain perfusion SPECT using 99mTc-labelled radiopharmaceuticals. *Eur J Nucl Med Mol Imaging.* 2009;36(12):2093-102.
23. Li R, Chen K, Wang Y, et al. Magnetic resonance-based attenuation correction in PET/MRI: comparison of segmentation-based and atlas-based methods. *Quant Imaging Med Surg.* 2018;8(2):141-8.
24. Shidahara M, Watabe H, Kimura Y, et al. PET kinetic analysis: Pitfalls and a solution for the Logan plot. *Ann Nucl Med.* 2003;17(6):407-14.